2014

Optimization of EHL Lubrication Performance in Thrust Slide-Bearings of Scroll Compressors

Noriaki Ishii
Osaka Electro-Communication University, Japan, ishii@isc.osakac.ac.jp

Takuma Tsuji
Mayekawa MFG. Co., Ltd., takuma-tsuji@mayekawa.co.jp

Keiko Anami
Ashikaga Institute of T, k.anami@nifty.com

Charles W. Knisely
Bucknell University, US, knisely@bucknell.edu

Katsunori Kurihara
Osaka Electro-Communication University, Japan, kstockme@purdue.edu

See next page for additional authors

Authors
Noriaki Ishii, Takuma Tsuji, Keiko Anami, Charles W. Knisely, Katsunori Kurihara, Tatsuya Oku, Kiyoshi Sawai, Hirofumi Yoshida, and Hiroaki Nakai

Optimization of EHL Performance in Thrust Slide-Bearings of Scroll Compressors

Noriaki ISHII[1]*, Takuma TSUJI[2], Keiko ANAMI[3], Charles W. KNISELY[4], Katsunori KURIHARA[1], Tatsuya OKU[2], Kiyoshi SAWAI[5], Hirofumi YOSHIDA[6] and Hiroaki NAKAI[6]

[1] Osaka Electro-Communication Univ., Dept. of Mechanical Engineering,Osaka, Japan.
Tel/fax: +81-72-820-4561, E-mail: ishii@isc.osakac.ac.jp

[2] Research and Development Center, Mayekawa MFG. Co., Ltd., Ibaraki, Japan,
E-mail: tatsuya-oku@mayekawa.co.jp

[3] Ashikaga Institute of Technology, Dept. of Mechanical Engineering, Tochigi, Japan.
E-mail: anami@ashitech.ac.jp

[4] Bucknell Univ., Dept. of Mechanical Engineering, Lewisburg, Pennsylvania, USA.
E-mail: knisely@bucknell.edu

[5] Dept. of Mechanical Engineering, Hiroshima Institute of Technology, Hiroshima, Japan.
E-mail: sawai@me.it-hiroshima.ac.jp

[6] Air-Conditioning and Cold Chain Development Center, Corporate Engineering Division Appliances Company, Panasonic Corporation, Shiga, Japan.
E-mail: yoshida.hirofumi @jp.panasonic.com

ABSTRACT

The present study focuses on aspects of EHL that have both positive and negative effects on the lubrication performance of the thrust slide-bearings in scroll compressors. Theoretical calculations using the average Reynolds equation of Patir-Cheng and the solid contact theory from Greenwood & Williamson, for the boundary of the local elastic deformation of the thrust slide-bearing, were conducted for a small cooling capacity scroll compressor driven at 3600 rpm with 0.1 kW. An approximate method was developed using characteristic curves to determine the oil film axial force, the average oil film thickness, the friction force and the friction coefficient. The calculations considered a variety of pressure differences due to the operating pressure and the thickness of thrust plate. Also, cases with a fixed uniform wedge angle at the periphery were calculated. The calculated results suggest a possible maximum reduction in friction coefficient of about 55% compared to that with a fixed uniform wedge angle. The reduction rate increases with decreasing thrust plate thickness, which, however, restricts the operating pressures to a lower pressure range. Design guidelines for optimizing EHL are suggested.

Key Words : Friction Coefficient, EHL, Optimization, Thrust Slide-Bearing, Scroll Compressor

1. INTRODUCTION

Previous studies by Ishii *et al*. (2008) and Oku *et al*. (2008) revealed the formation of a uniform oil wedge at the periphery of the thrust plate of the thrust slide-bearing in scroll compressors. This oil wedge results from the uniform elastic deformation of the orbiting thrust plate due to the pressure difference across the orbiting thrust plate (see Figure 1a). It is a significant factor in the high oil film pressure in the uniform wedge (see Figure 1b), the distribution of which is color-contoured-displayed in Figure 1(c), thus resulting in a high lubrication performance. In addition, the high oil film pressure also induces a local elastic deformation of the fixed thrust plate normal to its surface, as shown in Figure 1(d). The normal thrust plate deformation in the front area effectively forms an elasto-hydrodynamic-lubrication (EHL) front-pocket, even more effectively increasing the oil film pressure between the sliding surfaces, due to the envelopment of the oil, as confirmed in our companion

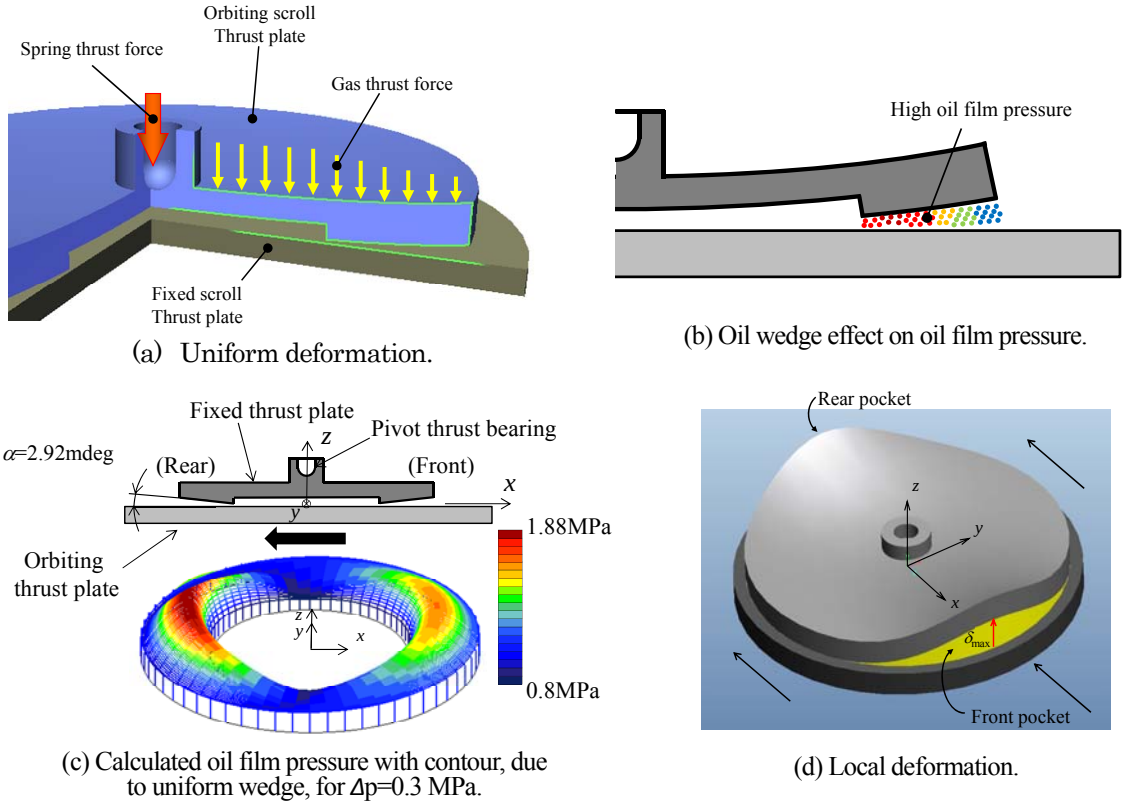

Figure 1 : Uniform and local elastic deformations of thrust slide-bearing.

paper by Ishii *et al*. (2014), and an earlier, less-detailed contribution by Ishii *et al*. (2012). The oil pressure formation in the rear pocket was confirmed to be unstable, as discussed by Ishii *et al*. (2014). Thus, the present study neglects the effect of the rear pocket and focuses on the EHL effect due only to the front pocket.

In the present study, the EHL effects on the lubrication performance of the thrust slide-bearings in a small cooling capacity scroll compressor driven at 3600 rpm with 0.1 kW are considered. The average Reynolds equation, the Patir & Cheng (1978, 1979) solid contact theory and the thrust plate equilibrium equation are calculated to quantify the oil film pressure changes relative to those with a uniform oil wedge angle, for a variety of the local elastic deformation and mean floating height of the thrust plate. Secondly, an approximate analysis method is developed using characteristic curves of the oil film pressure changes and the local elastic deformations to determine the mean floating height of the thrust plate. Thirdly, the approximate method is applied to soft-EHL analyses for a variety of the thrust plate thickness with a fixed uniform wedge angle. Then, the analysis considers a variety of the uniform wedge angle with a fixed thrust plate thickness, under a variety of pressure differences due to the operation pressure, thus determining the oil film axial force, the average oil film thickness, the friction force and the friction coefficient. In conclusion, the optimization of EHL performance is presented, suggesting a significant reduction in friction coefficient, compared to that with a fixed uniform wedge angle. Design guidelines for optimizing EHL are also suggested.

2. EHL-ANALYSIS FLOW CHART AND MAJOR SPECIFICATIONS FOR CALCULATIONS

A flow chart of theoretical analysis of lubrication at the thrust slide-bearing is shown in Figure 2, where the broken line shows the computation, made with soft EHL taken into account. Soft EHL refers to EHL in which there is no rigid surface to rigid surface contact as found on meshing gear teeth and the oil is assumed isothermal and incompressible. Initially, the bearing position (mean floating height h_0 and gradient angles ψ_x and ψ_y of the thrust plate) of the thrust plate is assumed, and the average Reynolds equation by Patir & Cheng (1978, 1979) is solved with the difference method (number of grids is 100 in the radial direction and 120 in the circumferential direction); the oil film force F_{OIL} and the oil film viscous resistance force F_{vs} are calculated, and subsequently the solid contact force F_{sc} and solid friction force F_{ss} are calculated, respectively. In the case that elastic deformation is taken into account, the elastic deformation of thrust plate, due to the oil film pressure, is calculated with FEM-analysis, for which the oil film height distribution and the oil film pressure are iteratively

computed until they converge. Furthermore, iterative computations are conducted for the bearing position, which was appropriately assumed, until the position converges.

The specifications of a small-sized scroll compressor for analysis are shown in Table 1. The motor shaft power was 0.1 kW. A ring-shaped thrust plate model of aluminum alloy, with the same area of 8772.5 mm^2 as that of the thrust bearing, had inside and outside radii of r_i =37.85 mm and r_o =65.0 mm, respectively. The pressure difference Δp between the outside and inside spaces of the thrust plate, representing the operating loads of the compressor, was varied from 0.1 MPa to 0.6 MPa. The thickness of the thrust plate varied from 10.4 mm to 40.0 mm and the wedge angle was fixed at 2.92 mdeg. The viscosity coefficient μ was assumed to be 0.0081 Pa·s for the mean temperature of 67.8°C and the mean pressure of 0.8 MPa. The orbiting speed N was 3600 rpm and the orbiting radius r_{obit} was 3.0 mm, resulting in a sliding speed V of 1.13 m/s.

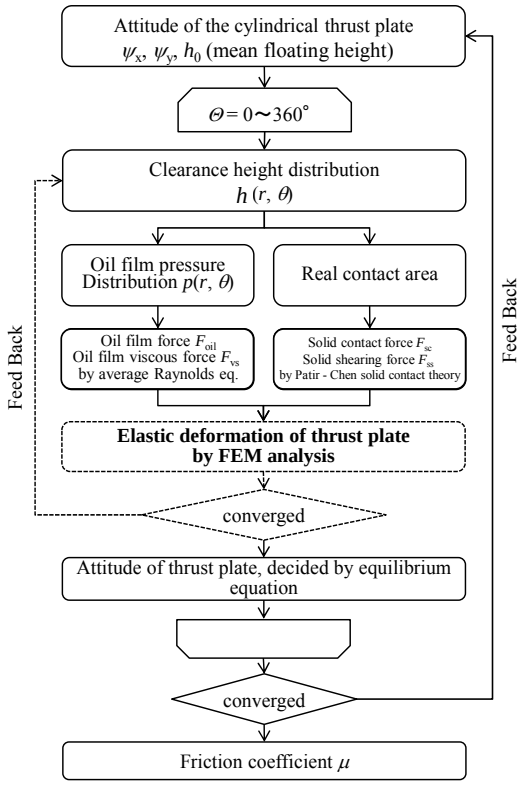

Figure 2 : Computation procedure for lubrication and attitude of thrust slide-bearing, without and with EHL pocket (dashed lines to be added for the case with EHL pocket)

Table 1 : Major specifications for computations for rigid thrust slide-bearing. model

Surface roughness R_a	Orbiting thrust plate [μm]	3.0
	Cylindrical thrust plate [μm]	0.056(in) ~ 0.27(out)
Standard deviation of surface roughness	Orbiting thrust plate σ_1 [μm]	1.458
	Cylindrical thrust plate σ_2 [μm]	0.188(in) ~ 1.15(out)
Bearing dimension	Outer radius r_o [mm]	65.0
	Inner radius r_i [mm]	37.85
	Friction surface area S_f [mm^2]	8772.5
Wedge angle α [mdeg]		2.92
Oil film thickness h_0 [mm]		~ 4.64 ~
Thrust plate thickness T_{th} [mm]		10.4
Pivot height L_{piv} [mm]		15.0
Cylindrical thrust plate mass m [kg]		0.340
Moment of inertia I_x, I_y [kg·m^2]		3.55×10^{-4}
Plastic flow pressure p_c [MPa]		1600
Shearing strength τ [MPa]		240
Surface density of asperities η [mm^{-2}]		400
Asperity summits radius β [μm]		8.0
Oil viscosity μ^* [Pa·s]		0.00702
Tenperature at the surface of thrust plate [°C]		70.0
Inner pressure p_{in} [Mpa]		1.0 ~ 0.8 ~ 0.5
Outer pressure p_{out} [MPa]		1.1
Pressure difference Δp [MPa]		0.1 ~ 0.3 ~ 0.6
Nominal gas thrust force F_p [kN]		~ 11.0 ~
Spring thrust force F_s [N]		600
Resultant thrust force F_T [kN]		~ 11.6 ~
Orbiting speed N [rpm]		3600
Orbiting radius r_{orb} [mm]		3.0
Sliding velocity V [m/s]		1.13
Number of grids	Radial	24
	Circumferential	120
Young modulus E [GPa]		73.5

3. EHL-POCKET OIL ENVELOPMENT EFFECTS UPON OIL FILM PRESSURE

From Figure 4 in our companion paper by Ishii *et al.* (2014), with a pressure difference Δp of 0.3 MPa and a mean floating height h_0 of the thrust plate of 4.64 μm, the uniform wedge angle at the periphery of the thrust plate, α, takes on the value of 2.92 mdeg. The corresponding front-side oil film pressure had a maximum pressure of 1.67 MPa. The thrust plate undergoes a local elastic deformation, in a pocket shape due to this high oil film pressure, as shown in Figure 1(d). FEM analysis was undertaken for a thrust plate thickness of 10.4 mm, to determine the circumferential distribution of elastic deformation, δ, shown in Figure 3(a), where the solid line shows the outer circumferential section and the broken line the inner circumferential section. The local elastic deformation occurs in the range of about ±110º. The local maximum deformation $\delta_{\max}$ appears at the front center section with values of 57 μm on the outer circumferential section and 28.5 μm on the inner circumference section (scale value on the left). The local elastic deformation decreases nearly linearly from the outer circumference towards the inner circumference. Our concern is focussed on how the oil film pressure is affected when the thrust plate undergoes orbiting motion with such a local elastic deformation.

With the thrust plate clearance height h_0 fixed at 4.64 μm for convenience, the oil film pressure was calculated with the average Reynolds equation, for the local elastic deformation δ, shown in Figure 3a, assuming the

occurrence of soft EHL with no changes in the viscosity and density of the lubricating oil. The abscissa represents the maximum local deformation height at the front center, δ_{max}. The calculated oil film representative pressure at the front center, p_{rep}, is plotted with an open circle (○) in Figure 3(b), taking on a value of 1.15 MPa at δ_{max} = 57 μm. This value is about 31% lower than the oil film representative pressure of 1.67 MPa (data plotted with a solid black circle (●)) at δ_{max} = 0 for no local elastic deformation (used as a reference point). This substantial decrease in oil film pressure is caused by the tunnel effect, which produces leakage of oil from the

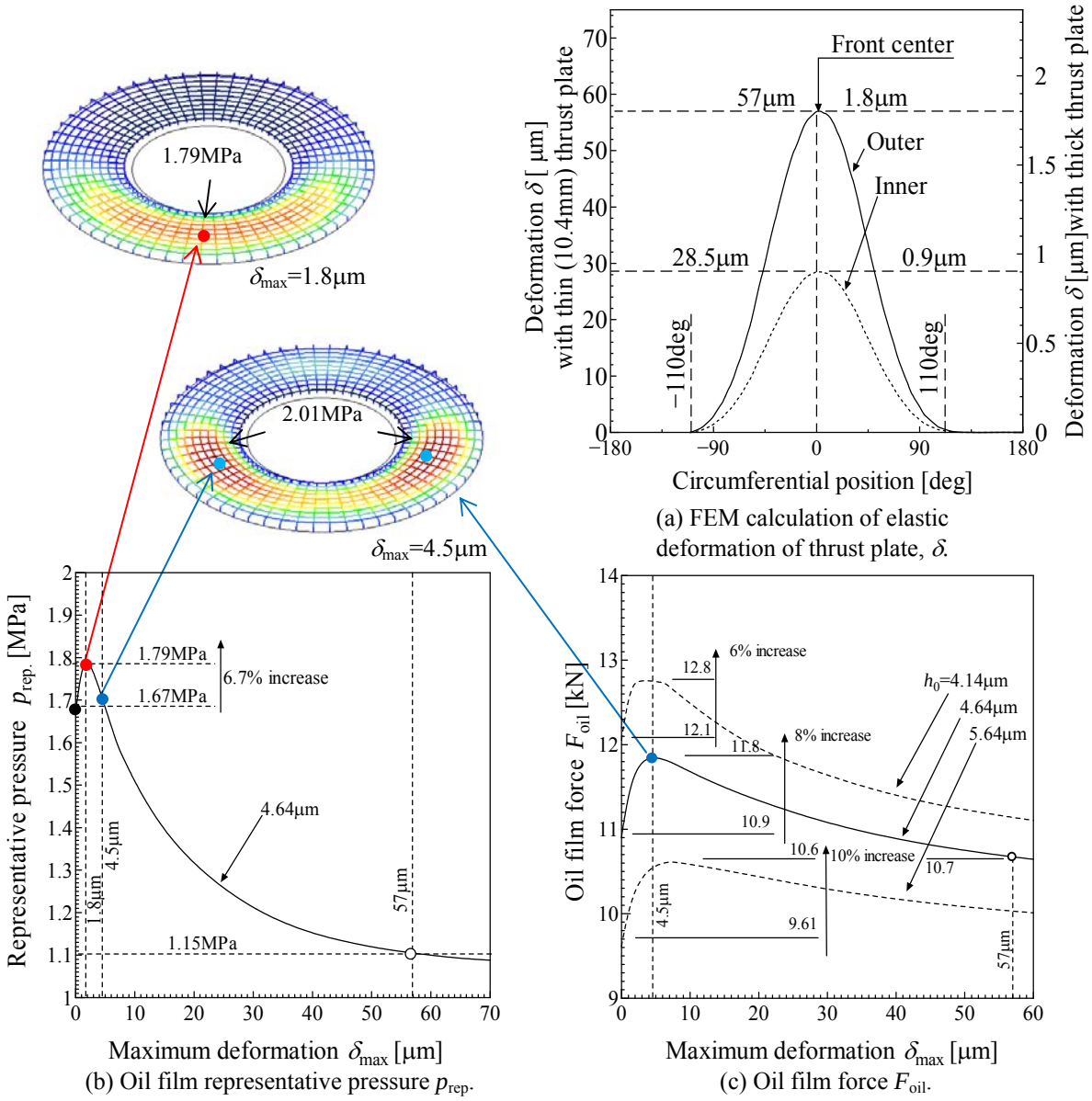

Figure 3 : Dependence of increase in oil film pressure and oil force due to oil envelopment with local elastic deformation, on maximum local deformation δ_{max} of thrust plate with uniform wedge angle α = 2.92 mdeg and mean floating height h_0 = 4.64 μm

large deformation in the inner circumference section of the thrust plate, thereby decreasing the oil envelopment effect.

On this basis, further calculations were made to determine how the oil film pressure changes with δ_{max}, the local elastic deformation shown in Figure 3(a), for a mean floating height h_0, fixed at the predetermined value of 4.64 μm. The decrease in the local elastic deformation was achieved by increasing the thrust plate thickness. As the maximum elastic deformation decreases from its initial value of 57 μm, in Figure 3(b), the oil film pressure gradually increases until it reaches a peak value of 1.70 MPa at δ_{max} = 1.8 μm. This representative pressure

value is 6.7% larger than the reference value of 1.67 MPa with no local elastic deformation. The corresponding deformation on the inner circumferential section was 0.9 μm, as shown by scale on the right in Figure 3(a).

A significant parameter is the oil film force F_{oil} and its behavior with decreasing maximum local elastic deformation δ_{max}. The oil film force F_{oil} can be calculated by integrating the oil film pressure distribution over the surface area. The resulting force is shown in Figure 3(c). At δ_{max} = 57 μm, F_{oil} takes on a value of 10.75 kN, which is approximately 2 % smaller than the reference value of 10.9 kN at δ_{max} = 0 μm. The oil film force F_{oil} achieves its maximum value of 11.8 kN at δ_{max} = 4.5 μm, which is 8 % larger than the reference value with that no local elastic deformation.

The peak of oil film force appears at δ_{max} = 4.5 μm, which is significantly larger than 1.8 μm for the oil film representative pressure peak. As shown in the contour diagram above Figure 3(b), the oil film pressure for δ_{max} = 4.5 μm splits at the front center. The representative pressure p_{rep} at the front center decreases, while the high pressure exhibits its maximum value of 2.14 MPa higher than 1.70 MPa for δ_{max} =1.8 μm, at both side of the thrust plate.

As shown by dotted lines in Figure 3(c), the oil film forces increases with decreasing the mean floating height h_0, while it decreases with increasing h_0.

4. SOFT-EHL ANALYSIS FOR THRUST SLIDE-BEARING

The flow chart for soft-EHL simulation was given in Figure 2. As indicated in the previous section, the oil film pressure in the sliding surface changes due to the local elastic deformation of the thrust plate. Consequently, the oil film force, acting upward on the thrust plate, changes and hence the mean floating height of the thrust plate, h_0, changes. With a change in the mean floating height, the upward directed oil film pressure changes, and thus the oil film force on the thrust plate changes to balance the downward resultant thrust force F_T of 11.6 kN caused by the pressure difference Δp of 0.3 MPa. In such a way, the mean floating height of the thrust plate, h_0, is determined. With this iterated state, the local elastic deformation of the thrust plate is re-calculated; then the oil film pressure and the mean thrust plate floating height are re-calculated, until they converge. With the converged solution determined, the friction coefficient can finally be calculated.

For such complicated iterative calculations, an approximate method, developed by Tsuji (2013), can be employed to achieve more readily the converged values. In the following section, this approximate method will be implemented for a uniform oil wedge angle α fixed at 2.64 mdeg, a pressure difference that is varied from 0.1 to 0.6 MPa, and a thrust plate thickness between 40 and 10.4 mm.

4.1 Simulation of Approximate Convergence Value for Mean Floating Height

The oil film force F_{oil} shown in Figure 3(c) is re-drawn in Figure 4, where the maximum elastic deformation of the thrust plate, δ_{max}, plotted on the abscissa, characterizes the upward convex deformation. The horizontal level shown by the broken line represents the standard oil film force, F_{oil_s}, the converged value of the thrust plate mean floating height for the uniform wedge model without the EHL effect denoted by h_0^{base}. This oil film force balances the downward resultant thrust load F_T. The solid line (black) represents the oil film force characteristic curve with EHL for the thrust plate mean floating height, fixed at h_0^{base}, representing the relation between the oil film force F_{oil_s} and the maximum deformation δ_{max}. This characteristic curve starts from F_{oil_s} at δ_{max} = 0 for no EHL effect and passes through the level of F_{oil_s}, as plotted by the black filled circle denoted by ⓪.

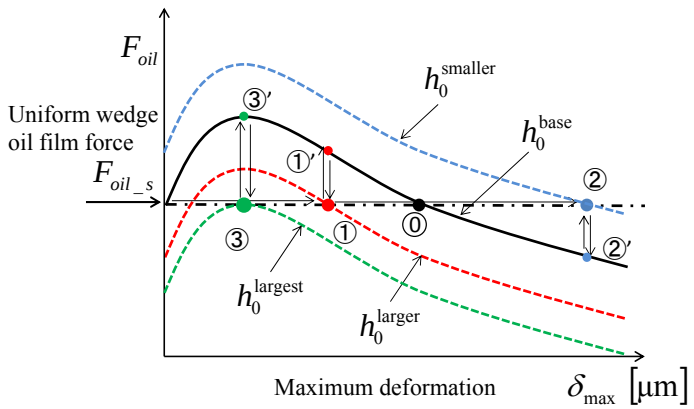

Figure 4 : Oil force dependence on local elastic deformation of thrust plate, for determination of mean floating height of thrust plate.

The maximum deformation δ_{max} depends upon both the thrust plate thickness and the oil film pressure. Three cases will be considered for the thrust plate maximum

deformation, for which an approximate thrust plate mean floating height h_0 can be determined :
Case 1: the thrust-plate maximum deformation is assumed to be at point ① (larger red circle) which is smaller than the point ⓪ for the base floating height h_0^{base}. With this maximum deformation, the oil film force increases as shown by the point ①' (smaller red circle), and is larger than the balancing oil film force F_{oil_s}. As a result, the thrust plate mean floating height h_0 increases to a value greater than h_0^{base}, so that the oil film force characteristic curve shifts downward, as shown by the dotted red line, and thus the oil film force balances the downward resultant thrust load. The thrust-plate mean floating height at this time, denoted by h_0^{larger}, is the converged approximate value, where $h_0^{larger} > h_0^{base}$.

Case 2: the thrust-plate maximum deformation is assumed to be at point ② (larger blue circle) which is larger than the point ⓪ for the base floating height h_0^{base}. With this maximum deformation, the oil film force decreases as shown by the point ②' (smaller blue circle), and is smaller than the balancing oil film force F_{oil_s}. As a result, the thrust plate mean floating height h_0 decreases to a value less than h_0^{base}, so that the oil film force characteristic curve shifts upward, as shown by the blue dotted line, and thus the oil film force again balances the downward resultant thrust load. The thrust-plate mean floating height at this time, denoted by $h_0^{smaller}$, is the converged approximate value, where $h_0^{smaller} < h_0^{base}$.

Case 3: the thrust-plate maximum deformation is assumed to be at point ③ (larger green circle) which is the deformation corresponding to the peak point of the characteristic curve. With this maximum deformation, the oil film force increases as shown by the point ③' (smaller green circle). In this case, the characteristic curve (black line) shifts to its maximum downward location, as shown by green dotted line, and the thrust-plate mean floating height is correspondingly at its greatest value, as denoted by $h_0^{largest} > h_0^{base}$.

As the thrust-plate mean floating height increases, the friction in the thrust bearing decreases, thus resulting in smaller coefficient of friction.

4.2 Simulation for Approximation of Local Elastic Deformation

The local elastic deformation of the thrust plate depends on the oil film pressure as well as on the thrust plate thickness; it can be calculated using FEM analysis, where the FEM model and major specifications for calculations are the same as those presented in detail in Section 4 in the companion paper by Ishii *et al.* (2014). In the FEM calculations of the thrust plate local elastic deformation, the oil film pressure is assumed to have the same distribution as that for the uniform oil wedge of 2.64 mdeg; the pressure amplitude is assumed to increase in proportion to the oil film representative pressure. FEM-calculated results in Figure 5 show the dependence of the characteristic curves of the oil film representative pressure, p_{rep}, on the resulting maximum deformation of

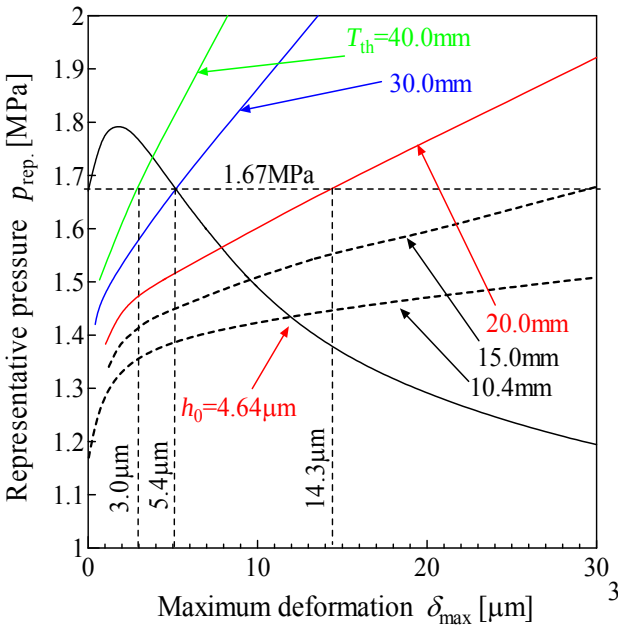

Figure 5 : Dependence of oil film representative pressure, p_{rep} on maximum deformation of thrust plate, δ_{max}, for Δp = 0.3MPa.

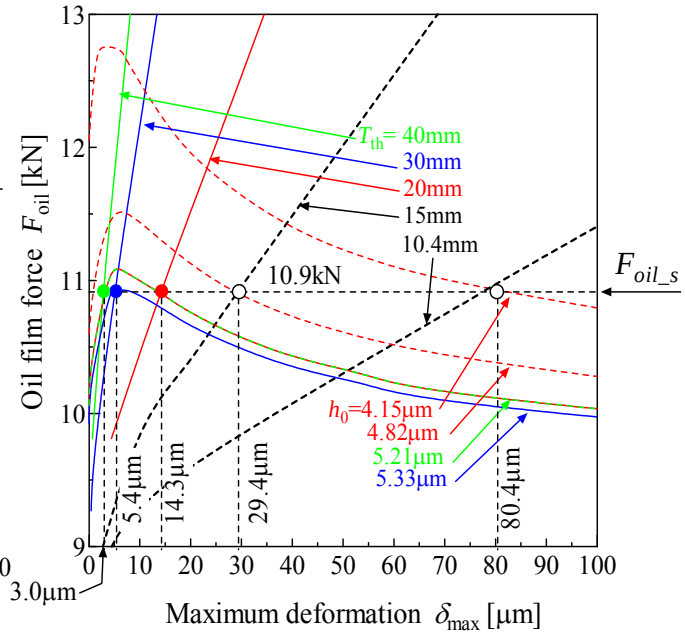

Figure 6 : Characteristic curves of oil film force and thrust plate elastic deformation for convergence approximation of thrust plate floating height, h_0, for Δp = 0.3MPa.

the thrust plate, δ_{max}. The parameter is the thrust plate thickness T_{th}, ranging from 10.4 mm to 40 mm. The black solid line is the characteristic curve for h_0 = 4.64 μm from Figure 3(b), and the horizontal line at 1.67 MPa is the oil film representative pressure with no EHL effect, that is, with a uniform oil wedge, which is also used for reference.

For all thrust plate thicknesses with deformations above 2 μm, the thrust plate deformation δ_{max} and the representative pressure p_{rep} are linearly related. The deformation δ_{max} at p_{rep} = 1.67 MPa is 3.0 μm for T_{th} =40 mm, 5.4 μm for T_{th} = 30 mm and 14.3 μm for T_{th} = 20 mm. However, the expected validity of present convergence approximation is limited to thrust plate deformations δ_{max} smaller than about 15 μm, at most.

4.3 Simulation for Approximation of Mean Floating Height

With the characteristic curves of the thrust plate local elastic deformation, shown in Figure 5, the approximate convergence value of the thrust plate mean floating height h_0 can be obtained by applying the fundamental concepts of the approximate method, as explained in Section 4.1. First, the characteristic curves of the oil film resultant force F_{oil} as functions of thrust plate elastic deformation δ_{max} are calculated, as shown in Figure 6, where the balancing oil film force F_{oil_s} is 10.9 kN with a pressure difference Δp of 0.3 MPa. The converged elastic deformations, plotted by the filled and open circles in Figure 6, correspond to the deformations in Figure 5 at which the characteristic curves cross the 1.67 MPa line. Now the thrust plate mean floating height h_0 for each plate thickness can determined by fitting the corresponding characteristic curves of the oil film force through the plotted data points along the F_{oil_s} = 10.9 kN line. The mean floating height h_0 was found to be 5.21 μm for both δ_{max} = 3.0 μm with T_{th}=40 mm and for δ_{max} = 14.3 μm with T_{th} = 20 mm; and h_0 = 5.33 μm at δ_{max} = 5.4 μm with T_{th} = 30 mm. The two unfilled data points at δ_{max} = 29.4 m and 80.4 μm exceed the range of deformations for which the approximate method is valid.

4.4 Major Characteristics of Lubrication with EHL Effect

Simulations similar to those presented in the previous section were performed for pressure differences Δp from 0.1 MPa to 0.6 MPa and for thrust plate thicknesses T_{th} from 10.4 mm to 40 mm to determine the thrust plate mean floating height h_0 (so-called "oil film thickness"). The calculated values for h_0 are shown by solid and dotted lines in Figure 7(a), where the bold dotted line represents the case with no EHL effect. The local elastic maximum deformation δ_{max} are shown in Figure 7(b). Once the mean oil film thickness is known, the major friction characteristics of the thrust slide-bearing with the uniform oil wedge angle α of 2.92 mdeg at its periphery can be calculated, and are shown in Figures 7(c) to 7(e).

The oil film viscous shearing force F_{vs} in Figure 7(c), shows that the inclusion of the EHL effect results in lower viscous friction than those without the EHL effect, over the whole range of pressure differences and for all thrust plate thicknesses. This improvement is believed to be due to the increased clearance of the sliding surfaces on the whole, due to the thrust plate elastic deformation. In contrast, the solid shearing force F_{ss}, shown in Figure 7(d), is essentially negligible for pressure differences Δp less than 0.3 MPa; it exhibits an increasing tendency over the range of Δp greater than 0.3 MPa. The solid shearing force for plates thicker than 30 mm are smaller than those with no EHL effect over the entire range of Δp considered. For plates thinner than 30 mm, the solid shearing force with EHL exceeds that without EHL curve at pressures that decrease with decreasing plate thickness (Δp of 0.51 MPa for T_{th} = 20 mm; 0.42 MPa for T_{th} = 15 mm; 0.31 MPa for T_{th} = 10.4 mm). This increase in solid shearing force is a consequence of the decrease in the bearing clearance h_0.

The friction force F_f , shown in Figure 7(e) and found as the sum of the viscous shearing force F_{vs} and the solid shearing force F_{ss}, exhibits values slightly smaller than with no EHL for the smaller pressure differences considered. This reduced total friction force is the effective positive EHL effect, induced by the oil envelopment. When the pressure difference Δp increases, however, the resultant friction force rapidly increases, exceeding the no EHL curve, due to the effect of increased solid shearing force. This increased total friction is a negative EHL effect, due to excessive elastic deformation. The critical value of Δp, at which the EHL effect shifts from a positive to negative factor increases with increasing plate thickness (0.34 MPa for T_{th} = 10.4 mm; 0.46 MPa for T_{th} = 15 mm; and 0.54 MPa for T_{th} = 20 mm). For plates thicker than 30 mm the negative EHL effect does not appear over the pressure differences considered.
The resultant friction force was used to calculate the coefficient of friction μ_{th} with the results shown in Figure 7(f), where the critical values of Δp for transition from a positive to negative EHL effect are the same as for the resultant friction force. For the pressure difference Δp = 0.1 MPa, the coefficient of friction μ_{th} is 0.01 for no

EHL curve, while it decreases to between 0.007 for T_{th} = 40 mm and 0.0045 for T_{th} = 10.5 mm, corresponding to a 30% to 55% decrease compared with that for no EHL effect. This is the positive EHL effect due to the oil envelopment. For the thrust plate thickness T_{th} greater than 30 mm, there appears no critical value at which μ_{th} exceeds that of the no EHL curve for the range of Δp considered. For plates thinner than 30 mm, the critical values correspond to those for total friction force.

Calculated results of friction coefficient present two significant suggestions for optimization of EHL performance. The first is to specify thinner the thrust plates in order to realize a larger positive effect of the oil envelopment phenomenon. However, it should be noted that the decrease in thrust plate thickness also results in a smaller range of the pressure differences over which the positive effect is achieved, that is, a smaller operating range. The second suggestion is to specify a thicker thrust plate with a reduced oil envelopment effect, but a more extended operating range.

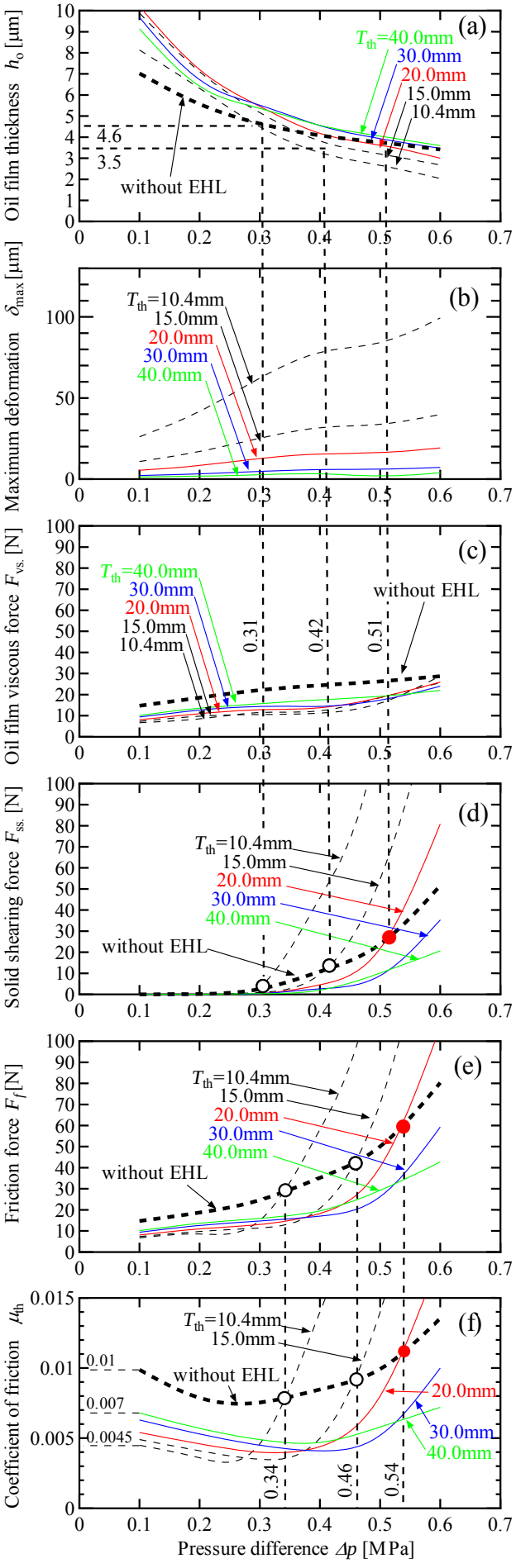

Figure 7 : Major friction characteristics with EHL effect on thrust slide-bearing with uniform oil wedge angle α of 2.92 mdeg at periphery as fucntions of pressure difference Δp:
(a) Mean floating height h_0 (oil film mean thickness);
(b) Local elastic maximum deformation δ_{max};
(c) Oil film viscous shearing force F_{vs};
(d) Solid shearing force F_{ss};
(e) Resultant friction force F_f ;
(f) Coefficient of friction μ_{th}.

5. CONCLUSION

A fundamental computation of the EHL effects was included in the lubrication analysis of the thrust slide-bearing of a compact scroll compressor with a motor shaft output of 0.1 kW. The intent was to determine the fundamental significant characteristics of the EHL effects on the high performance in lubrication of the thrust slide-bearing. Several simplifying assumptions were necessary in this first step of soft-EHL analysis. The results are as follows:

(1) For a small pressure difference of 0.1 MPa, corresponding to low load operation of scroll compressors, a significantly larger oil film force is induced with the inclusion of the EHL effect than that when EHL effect is omitted for all thrust plate thicknesses. The thrust bearing floating height increases correspondingly. As a result, the coefficient of friction significantly decreases relative to that with no EHL effect, from a 30% reduction for the thrust plate thickness T_{th} = 40 mm to a 55% reduction for T_{th} =10.4 mm, with intermediate reductions for intermediate plate thicknesses.

(2) For a large pressure difference of 0.6 MPa, corresponding to high load operation of scroll compressors, the local elastic deformation can become excessive for thin thrust plates and hence the oil film force becomes smaller than that for no EHL effect, thus decreasing the thrust bearing floating height. With decreased floating height, the solid friction force increases and the coefficient of friction increases beyond that for no EHL effect. Attention should be paid to such cases where the EHL analysis shows that it can exert a negative effect on the lubrication in the thrust slide-bearing due to the elastic deformation of thrust slide-bearing.

(3) Specification of a thin thrust plate thickness will result in a large positive effect due to the oil envelopment in the EHL pocket. The range of the pressure differences over which the positive EHL effect was found to be operative in this study was limited to 0.1 MPa to 0.33 MPa. A thin thrust plate will have a negative EHL effect at high load operation.

(4) Specification of a thicker thrust plate decreases the positive oil envelopment effect to some extent but permits a wider range of high load operation. As a concrete target specification of a thrust plate thickness greater than 30 mm was found to reduce the coefficient of friction by about 30% compared with that for no EHL effect, over the full range of pressure differences from 0.1 MPa to 0.6 MPa considered in this study.

Lubrication analyses including the EHL effects could be conducted by computer calculations with introduction of compliance matrix and so on. However, the compliance matrix for the thrust slide-bearing was hard to develop at present. For this reason, an approximate method was employed in the present study. The approximate method is quite readily implemented using computer-based calculations and provides a very clear and significant physical understanding. In the present computer-simulations with the approximate method, however, the convergence errors become unacceptably large for larger local elastic deformations of the thrust plate. Therefore, continued improvements are needed in these computer-simulations using the approximate method to compensate for simulation errors for larger deformations. Alternatively, computer calculations involving the introduction of compliance matrix should be developed.

The authors hope that the present study will serve to spur other investigators to consider the significance of the EHL effect in the thrust slide-bearing of scroll compressors and to initiate their own investigations in order to gain an clear understanding of the essential mechanism of high lubrication performance that scroll compressors possess. Such widespread efforts will permit the development of super scroll compressors with higher performance and greater reliability.

NOMENCLATURE

F_f : Resultant frictional force, N
F_{oil} : Oil film force, N
F_{oil_s} : Standard oil film force, N
F_s : Axial spring force, N
F_{ss} : Solid shearing force, N
F_T : Resultant thrust force, N
F_{vs} : Oil viscous force, N
h_0 : Average clearance height, m
N : Orbital speed, rpm
p : Oil film pressure, Pa
p_{rep} : Oil film representative pressure, Pa
r_i, r_o : Inner bearing radius, m
T_{th} : Thrust plate thickness, m

α : Wedge angle, rad
δ : Elastic deformation height, μm
δ_{max} : Maximum deformation height, μm
Δp : Pressure difference, Pa
Θ : Orbiting angle, rad
μ_{th} : Coefficient of friction, -
μ^* : Oil viscosity, $Pa \cdot s$
ψ_x, ψ_y : Rotation angle rotating x - axis, rad

REFERENCES

Ishii, N., Oku, T., Anami, K., Knisely, C.W., Sawai, K., Morimoto, T., Iida, N., 2008, Experimental Study of the Lubrication Mechanism for Thrust Slide Bearings in Scroll Compressors, *An International Journal of Heating, Air-Conditioning and Refrigerating Research (HVAC&R Research), ASHRAE*, **Vol.**14, No.3: p.463 - 435

Ishii, N., Tsuji, T., Oku, T., Anami, K., Knisely, C.W., Nokiyama, K., Morimoto, T., Sakuda, A., Sawai, K., 2012, "Elasto-Hydrodynamic Lubrication Effect in Thrust-Slide Bearings of Scroll Compressors," *2012 Purdue Conference Paper (Paper 1438).*

Ishii, N., Tsuji, T., Anami, K., Nokiyama, K., Yoshida, H., Nakai, H., Oku, T., Sawai, K., Knisely, C.W., 2014, "Hydrodynamic-Pressure-Induced Elastic Deformation of Thrust Slide-Bearings in Scroll Compressors and Oil Film Pressure Increase Due to Oil Envelopment," *submitted to 2014 Purdue Herrick Conferences.*

Oku, T., Ishii, N., Anami, K., Knisely, C.W., Sawai, K., Morimoto, T., Hiwata, A., 2008, Theoretical Model of Lubrication Mechanism in the Thrust Slide-Bearing of Scroll Compressors, *An International Journal of Heating, Air-Conditioning and Refrigerating Research (HVAC&R Research), ASHRAE*, Vol.14, No.2: p.239-358.

Patir, N. and Cheng, H. S., 1978, An Average Flow Model for Determining Effects of Three-Dimensional Roughness on Partial Hydrodynamic Lubrication, *Transaction of the ASME, Journal of Lubrication Technology,* Vol. 100, No. 1: p. 12-17.

Patir, N. and Cheng, H. S., 1979, Application of Average Flow Model to Lubrication Between Rough Sliding Surfaces, *Transaction of the ASME, Journal of Lubrication Technology,* Vol. 101, No. 2: p. 200-229.

Tsuji, T., 2014, "A Study of Refrigerant Compressors for Higher Performance, Part 1: Design Guideline for Performance Optimization of Reciprocating Compressors; Part 2: Oil Envelopment Phenomenon in Thrust Slide-Bearing of Scroll Compressors and Soft EHL Analysis," *Doctoral Thesis*, presented to Osaka Electro-Communication University.

ACKNOWLEDGMENT

The authors wish to thank Professor Hiroshi Yabe at Electro-Communication University, Mr. Shuichi Yamamoto, Senior Councilor, R&D Division, Panasonic Co., Ltd., Mr. Kiyoshi Imai, Vice President, Corporate Engineering Division, Appliances Company, Panasonic Corporation, and Mr. Masahiro Atarashi, Director, Appliances Company, Panasonic Corporation for their encouragement and valuable assistance in carrying out this work and their permission to publish this study.